New Journal of Physics
The open access journal at the forefront of physics
Deutsche Physikalische Gesellschaft DPG | IOP Institute of Physics

Importance of *d–p* Coulomb interaction for high T_C cuprates and other oxides

P Hansmann[1], N Parragh[2], A Toschi[3], G Sangiovanni[2] and K Held[3]
[1] Centre de Physique Théorique, Ecole Polytechnique, CNRS-UMR7644, F-91128 Palaiseau, France
[2] Universität Würzburg, Am Hubland, D-97074 Würzburg, Germany
[3] Institut für Festkörperphysik, Vienna University of Technology, A-1040 Vienna, Austria
E-mail: philipp.hansmann@googlemail.com

Received 10 December 2013, revised 3 February 2014
Accepted for publication 10 February 2014
Published 7 March 2014
New Journal of Physics **16** (2014) 033009
doi:10.1088/1367-2630/16/3/033009

Abstract
Current theoretical studies of electronic correlations in transition metal oxides typically only account for the local repulsion between *d*-electrons even if oxygen ligand *p*-states are an explicit part of the effective Hamiltonian. Interatomic interactions such as U_{pd} between *d*- and (ligand) *p*-electrons, as well as the local interaction between *p*-electrons, are neglected. Often, the relative *d–p* orbital splitting has to be adjusted 'ad hoc' on the basis of the experimental evidence. By applying the merger of local density approximation and dynamical mean field theory to the prototypical case of the three-band Emery *dp* model for the cuprates, we demonstrate that, without any 'ad hoc' adjustment of the orbital splitting, the charge transfer insulating state is stabilized by the interatomic interaction U_{pd}. Our study hence shows how to improve realistic material calculations that explicitly include the *p*-orbitals.

Keywords: correlated electrons, dynamical mean field theory, transition metal oxides

1367-2630/14/033009+16$33.00

1. Introduction

A primary effect of electronic correlations is to turn materials, which according to band-theory would be metallic, into insulators classified as Mott–Hubbard and charge transfer insulators [1]. Experimentally, various transition metal oxides were intensively investigated [2]. The huge interest in this subject goes back to the unexpected discovery [3] of high-temperature superconductivity, by doping the charge transfer insulating cuprates. On the theoretical side, great efforts to solve the Hubbard model [4] have been made since this model captures, in a fundamental way, the competition between electronic mobility and localization, generated by a purely local interaction.

No exact solution of the Hubbard model in two or three dimensions is known hitherto, but a breakthrough was achieved by dynamical mean field theory (DMFT) [5–7]. DMFT extends the concept of a mean field theory to quantum mechanics and takes into account, non-perturbatively, a major part of the electronic correlations, i.e. the local electronic correlations in time. A further, and significant, advantage of DMFT is the possibility to combine it with *ab initio* density functional calculations, e.g. with the local density approximation (LDA) in the so-called LDA+DMFT [8] approach, which has already evolved to a considerable maturity. By means of LDA+DMFT, realistic calculations of correlated materials with a high degree of accuracy became possible, as is exemplified well by the successful treatment of the Mott–Hubbard transition in V_2O_3 [9].

The high-temperature superconducting cuprates obviously represent a much more challenging case for DMFT-based methods. In fact, the extremely anisotropic (quasi two dimensional) layered structure of these compounds enhances the importance of *non-local* spatial correlations. Hence, if aiming at the low-temperature physics of cuprates, non-local correlations need to be taken into account, which could be achieved by cluster [10] or diagrammatic extensions [11] of DMFT. Here, we are not focusing on if, or to what extent, the Hubbard model describes the unconventional superconductivity of the cuprates—a question on which no consensus has been reached yet. Instead, we will focus on the analysis of the high-temperature regime of the undoped cuprates. Since the effect of non-local correlations will be gradually mitigated by temperature [12–14], employing LDA+DMFT is more justified. LDA+DMFT was already successfully applied to the cuprates for analyzing the anomalies in the restricted optical sum rules [15–18] and the fingerprints of the Zhang–Rice physics in photoemission spectra [22, 23]. Here, we will employ LDA+DMFT[4] to investigate the fundamental nature of the high-temperature insulating state in the undoped compounds. This insulating state, classified as a charge transfer insulator [2], is in fact common for many transition metal oxides. A crucial step in the LDA+DMFT method is the derivation of the low-energy Hamiltonian from *ab initio* calculations by renormalization (downfolding [24]) to certain basis states around the Fermi energy. The decision on the basis, in fact, is crucial. For the cuprates this question basically boils down to include oxygen $2p$ ligand-states explicitly or implicitly. The simplest possible Hamiltonian with both Cu $3d$ and oxygen $2p$ states is the Emery model which includes, besides the Cu $x^2 - y^2$ band, the strongest hybridizing p_x and p_y

[4] Specifically, for all the DMFT and DMFT+Hartree calculations presented in this work the Würzburg–Wien 'w2dynamics' code [19], exploiting the hybridization-expansion implementation [20] of the continuous-time quantum Monte Carlo method [21], has been used.

states in the xy plane (an extensive discussion on the downfolding procedure for cuprates can be found in [32]).

In the renormalization sense, physical observables of different effective Hamiltonians should coincide at low energies, albeit the larger effective Hamiltonians might be more accurate than those defined on narrower energy windows. By extending the basis-set, one (i) enlarges the energy range and the physical processes explicitly included in the downfolding procedure, and (ii) obtains a better localization of the more correlated d-orbitals. Such a general statement is however premature if the extension exclusively relies on the one-particle (kinetic) part of the Hamiltonian. One should not forget that the Coulomb interaction needs to be renormalized as well.

The material best studied in LDA+DMFT within different basis-sets is arguably $LaNiO_3$, and heterostructures thereof. Here, including the p-states in a dp-model [26] leads to qualitatively different results compared to the d-only model [27]. As pointed out in [28], the physics is very different in both cases: in the dp-model the d-occupancy is larger with a tendency of two d-electrons to form a spin-1 due to Hund's exchange. On the contrary, the d-only model is built with a (fixed) d^1 configuration. In such a situation, it is pretty unclear whether the dp-model does actually provide a more accurate description of the physics, as one might naively expect due to the larger number of degrees of freedom explicitly taken into account within the larger basis-set of the downfolded model [29].

Hitherto, the additional oxygen p-orbitals in the extended basis-sets have been considered as *not* interacting in state-of-the-art LDA+DMFT calculations, i.e. only a local d–d interaction has been taken into account. While the oxygen p-orbitals are, due to their nodeless radial wave function also quite localized, their typical filling in transition metal oxides renders the onsite p-interaction to be non-crucial. Yet, at the same time, our numerical results show that the effect of the *interatomic* $2p$–$3d$ interaction, in the following coined as U_{pd}, *does* have a large effect. U_{pd} is an essential parameter that controlls the metal-to-insulator transition, as well as the size of the charge transfer gap.

The paper is organized as follows: in section 2 the construction of the Emery model is described starting from the full LDA bandstructures. Section 3 and the appendix are dedicated to the DMFT and Hartree treatment of the various Coulomb interactions. Section 4 presents the results obtained, in particular the opening of the charge transfer gap and the importance of U_{pd} to this end. Finally, section 5 summarizes the paper.

2. The Emery model revisited

A popular tight-binding Hamiltonian for the high T_C cuprates, including oxygen p-states, is a three-band model suggested by Emery [30] in 1987. The Emery model consists of one planar Cu $x^2 - y^2$ band, two oxygen p_x and p_y bands and takes into account a d–p hopping, see table 1. It is thus the minimal model in order to describe the charge transfer insulating state and, moreover, the physics of a Zhang–Rice singlet [31]. These features are obviously beyond a description of the cuprates within an effective single band model. However, Andersen *et al* [32] concluded from downfolding the *ab initio* LDA bandstructure that the original model as described in [30] should be extended. These extensions originate basically from the inclusion of an *axial* degree of freedom (including mostly Cu 4 s-states and apical oxygen states) which was

Table 1. Extended Emery model [35] including *p–p* hopping mediated by the *material dependent* axial degree of freedom.

$$\hat{H}^{\mathrm{NMTO}} = \sum_{klm\sigma} h^{\mathrm{LDA}}_{lm}(\mathbf{k}) c^{\dagger}_{l\sigma}(\mathbf{k}) c_{m\sigma}(\mathbf{k})$$

$$h_{\mathrm{NMTO}}(\mathbf{k}) \begin{pmatrix} h_d(\mathbf{k}) & h_{d,px}(\mathbf{k}) & h_{d,py}(\mathbf{k}) \\ h_{px,d}(\mathbf{k}) & h_{px}(\mathbf{k}) & h_{px,py}(\mathbf{k}) \\ h_{py,d}(\mathbf{k}) & h_{py,px}(\mathbf{k}) & h_{py}(\mathbf{k}) \end{pmatrix}$$

$$\begin{aligned}
h_d(\mathbf{k}) &= \varepsilon_d + 2\mathrm{t}_{dd}(\cos(k_x) + \cos(k_y)) + 4\mathrm{t}'_{dd}\cos(k_x)\cos(k_y) \\
h_{px}(\mathbf{k}) &= \varepsilon_p + 2.0(\mathrm{t}'_{pp}\cos(k_x) + \mathrm{t}''_{pp}\cos(k_y) + 2\mathrm{t}'''_{pp}\cos(k_x)\cos(k_y)) \\
h_{py}(\mathbf{k}) &= \varepsilon_p + 2.0(\mathrm{t}'_{pp}\cos(k_y) + \mathrm{t}''_{pp}\cos(k_x) + 2\mathrm{t}'''_{pp}\cos(k_y)\cos(k_x)) \\
h_{d,px}(\mathbf{k}) &= 2((\mathrm{t}_{pd} + 2\mathrm{t}'_{pd}\cos(k_y))\sin(k_x/2) + (\mathrm{t}''_{pd} + 2\mathrm{t}'''_{pd}\cos(k_y))\sin(3k_x/2)) \\
h_{d,py}(\mathbf{k}) &= -2.0((\mathrm{t}_{pd} + 2\mathrm{t}'_{pd}\cos(k_x))\sin(k_y/2) + (\mathrm{t}''_{pd} + 2\mathrm{t}'''_{pd}\cos(k_x))\sin(3k_y/2)) \\
h_{px,py}(\mathbf{k}) &= -4.0(\mathrm{t}_{pp}\sin(k_x/2)\sin(k_y/2) + \mathrm{t}''''_{pp}(\sin(3k_x/2)\sin(k_y/2) \\
&\quad +\sin(3k_y/2)\sin(k_x/2)))
\end{aligned}$$

seen to describe the material dependence of the electronic structure in the cuprates [33]. The derivation starts from eight bands which are separated into a 4×4 σ-bonding block of Cu $3d_{x^2-y^2}$, O_1 $2p_x$, O_2 $2p_y$, as well as Cu 4 *s* (with some Cu $3d_{3z^2-r^2}$ character), and another 4×4 π-bonding block of Cu-$3d_{xz}$, Cu $3d_{yz}$, O_1 $2p_z$ and O_2 $2p_z$. The generic Hamiltonian for the CuO_2 planes is the 4×4 σ-block, since it contains the conduction band. Due to symmetry reasons, the σ- and the π-block do not hybridize in the limit of *flat planes* [32].

Starting from the four band σ-Hamiltonian one can arrive either at (i) a two-band Hamiltonian with *planar* ('dressed' Cu $x^2 - y^2$) and *axial* ('dressed' Cu 4 *s*) degrees of freedom[5], or at (ii) the three-band Emery model. The latter is obtained by folding the *axial* degrees of freedom down to the oxygen bands, resulting in an additional (material dependent) *p–p* hopping t_{pp} and renormalization of the onsite *p*-energy.

Quantitative Hamiltonians can be obtained by means of *N*th order muffin tin orbitals (NMTO) [24] based on a Löwdin downfolding scheme with subsequent '*N*-ization' ($N = 0$: linearization). This technique has been already established and used in several LDA+DMFT calculations [25]. In our paper, we will consider two different low-energy Hamiltonians [34, 35]: the first one consists of $N = 0$ muffin tin orbitals which have been linearized around the Fermi energy. The 0MTO basis gives correct LDA wave functions at the Fermi level and, by virtue of the variational principle, the correct LDA Fermi surface and Fermi velocities. The 1MTO basis gives, in addition to this, the correct LDA wave functions at an energy $E1$ chosen at the bottom of the *pd*-bonding band, and hence, the correct $E(k) = E1$ surface and velocities. The resulting Hamiltonian can be written analytically as in table 1 with hopping parameters given in table 2.

In figure 1 we show these NMTO downfolded bands for La_2CuO_4 from Kent *et al* [35] for $N = 0$ (linearization around the Fermi energy—left-hand side) and $N = 1$ (with E_1 chosen to be at the bottom of the *pd*-bonding band at (π, π)—right-hand side). The corresponding hopping

[5] In this case the σ-oxygen states fold into the *planar* $x^2 - y^2$ conduction band.

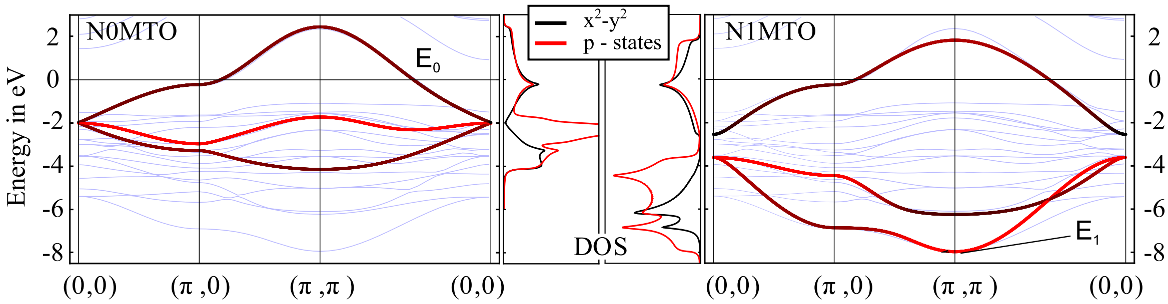

Figure 1. Bandstructure and single particle density of states for the 0MTO and 1MTO downfolded model [34, 35]. The color codes the orbital character: 3d $x^2 - y^2$ is black, whereas the p-states are summarized and plotted in red (gray)-color mixing corresponds to a mixed orbital state. The LDA bands are shown as thin (blue) lines.

Table 2. Hopping integrals for the Emery model table 1 as obtained by 0MTO and 1MTO in [34, 35].

NMTO	$\varepsilon_d - \varepsilon_p$	t_{dd}	t_{pd}	t'_{pd}	t_{pp}	t'_{pp}	t''_{pp}	t'''_{pp}
N = 0	0.43	-0.10	0.96	-0.10	0.15	-0.24	0.02	0.11
N=1	0.95	0.15	1.48	0.08	0.91	0.03	0.15	0.03

parameters can be found in table 2. The difference of the $N = 0$ and $N = 1$ models is the energy range in which they reproduce the cuprate LDA bandstructure (light blue lines): while the $N = 0$ model only has one fixed energy, namely the Fermi energy E_{F}, the $N = 1$ model was fixed to ε_{F} and to the energy of the bottom of the bonding pd-bands at around -8 eV. By having to span a wider energy range, the $N = 1$ orbitals are somewhat less localized, and consequently have longer-ranged hoppings than the $N = 0$ orbitals. A thorough discussion on the relations and trends of the hopping parameters can be found in [35] and [34]. In our study we will consider first the $N = 0$ and then the $N = 1$ model in order to address the following issue of central interest: the most problematic step in recent studies [37, 38] was the value of the d–p splitting $\varepsilon_d - \varepsilon_p = \Delta_{dp}$. While the NMTO downfolding [35] yields a value of $\Delta_{dp} = 0.45$ eV ($N = 0$) or $\Delta_{dp} = 0.96$ eV ($N = 1$), it turns out that the many-body treatments, which include correlation effects fail to reproduce the insulating behavior of the undoped LSCO. In order to fix this problem Δ_{dp} was increased 'by hand' to values of the order of $\Delta_{dp} \approx 3$ eV [35, 38] or it was chosen as a variable parameter [37]. Further, Kent *et al* [35] pointed out that previous justifications of such enhancement of Δ_{dp} by means of constrained LDA calculations for La_2CuO_4 are problematic due to a misleading assumption of the electron count. Our analysis in the subsequent sections will clarify, how these problems are actually related to the assumption of negligible Coulomb interactions between d and p-electrons in the many-body calculations.

3. Methods: *dp*-models in DMFT+Hartree

We supplement the one-particle extended Emery model from table 1 by the following two-particle interactions

$$H_U = U_{dd}\sum_i n_{id\uparrow}n_{id\downarrow} + U_{pp}\sum_j n_{jp_j\uparrow}n_{jp_j\downarrow} + U_{pd}\sum_{\langle ij\rangle\sigma\sigma'} n_{id\sigma}n_{jp_j\sigma'}. \tag{1}$$

Here i and j sum over all Cu and O sites, respectively; $p_j \in \{p_x, p_y\}$ denotes the particular p-orbital we include on a given O site j in the Emery model; $\langle ij\rangle$ denotes the restriction to nearest neighbors, i.e. a Cu site i and its four surrounding O sites j; and $n_{il\sigma} = c^\dagger_{il\sigma}c_{il\sigma}$. This way the most important (largest) interaction parameters are included: the local Coulomb interactions on the Cu (U_{dd}) and O sites (U_{pp}) and the nearest neighbor Cu–O interaction U_{pd}.

Since part of H_U is contained in the NMTO one-particle energies, we need a so-called double counting corrections (DC). For the dp-models, the DC effect is much more important than for d-only models where it often corresponds to a simple energy shift that can be 'absorbed' by the chemical potential. We employ the Anisimov DC formula [39] (also coined as fully localized limit) and extend it straightforwardly to the dp-basis:

$$\Delta\varepsilon^{d(p)}_{\mathrm{DC}} = U_{dd(pp)}\left[n_{d(p)} - \frac{1}{2}\right] + 4(2) \times U_{pd}\, n_{p(d)}. \tag{2}$$

Here, $n_{d(p)}$ are the LDA density for the $d(p)$-orbitals (Cu (O) sites have four O (Cu) neighbors). So the DC corresponds to a relative shift between the d and p-states, which would be reversed by a simple mean field treatment of U_{dd} U_{pd}, and U_{pd}.

Let us emphasize that, in contrast to standard LDA+DMFT implementations [28], we treat *all* density–density interactions within the dp basis in DMFT+Hartree. Specifically, U_{dd} is treated in DMFT (CTQMC) where we define a local Anderson impurity model from the local Cu d Green function and self-energy. The interactions U_{pp} and U_{pd} are treated on the Hartree level, i.e. a self-energy contribution for each d- and p-site is calculated as $U_{pp}(U_{pd})$ times the density of the other orbitals involved. Please note that if $n_{d(p)}$ remained at its LDA value the DC term would cancel the effect of U_{pd} in DMFT+Hartree exactly. However, due to the electronic correlations, in particular due to the splitting of the d-orbitals, n_d is reduced and n_p enhanced. In a fully charge self-consistent LDA+DMFT calculation, part of this U_{pd} effect is transferred to the LDA part. Coming closer to our treatment would be a charge self-consistent LDA+U+DMFT scheme, where '+U' (Hartree) is taken into account for U_{pd} and in particular U_{pp} and '+DMFT' for U_{dd}.

Let us note that for U_{pd} the Hartree treatment is exact in the DMFT limit since non-local interactions reduce to their Hartree contribution, see [40]. In the case of U_{pp}, a DMFT solution for the O sites would be in principle required, exactly as for the Cu site. However, since the p-orbitals are almost completely filled, electronic correlations are actually weak and the simpler Hartree treatment well reproduces the DMFT solution, as we explicitly show in appendix. Our approach incorporates therefore the advantages of the DMFT and explicitly keeps the p-degrees of freedom also in the interaction part of the many-body Hamiltonian. The extended basis-set allows us not only to capture Mott–Hubbard physics, but also that of charge transfer insulators and the concomitant d–p interplay. The latter is, in fact, the relevant one for the physics of undoped/underdoped cuprates.

Before turning to the results let us mention that the analytic continuation of the numerical LDA+DMFT results is more complicated for the extended dp basis-set. This issue is discussed in the appendix as well.

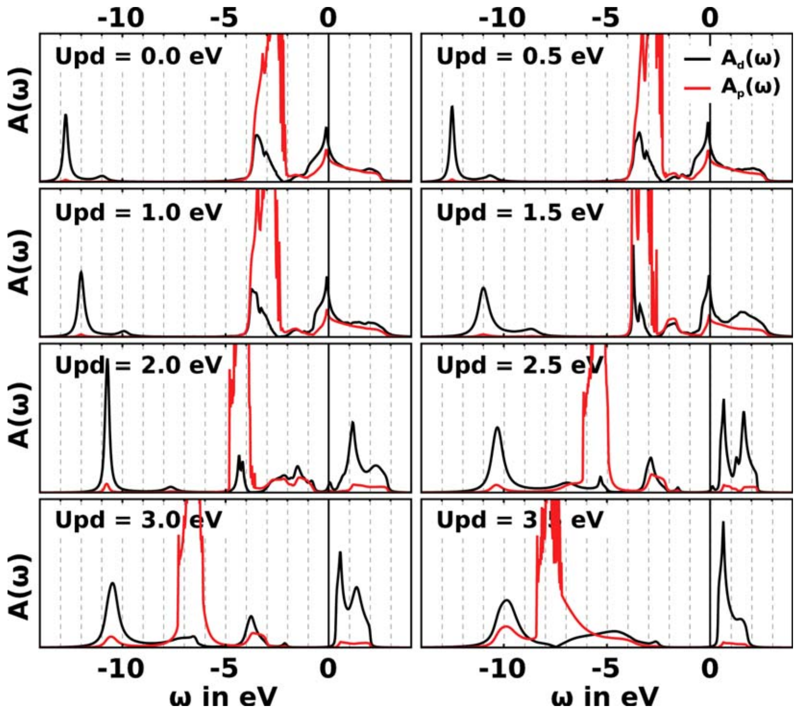

Figure 2. DMFT spectra for the 0MTO basis with interaction parameters $U_{dd} = 10\,\text{eV}$, $U_{pp} = 5\,\text{eV}$, and varying U_{pd}. The line at $\omega = 0$ denotes the Fermi level.

4. Results

Our DMFT+Hartree results for both 0MTO and 1MTO basis-sets can be summarized in two conclusions:

1. The d–p interaction U_{pd}, which leads to a *self-consistently determined* level shift, drives the system insulating within DMFT+Hartree and opens the charge transfer gap.
2. The critical interactions for this metal-to-insulator transition in 0MTO agree with estimates of the interaction strength; for 1NMTO they are at the upper borderline or somewhat larger than what can be expected.

0MTO model. For the interaction parameters of the 0MTO calculation we choose $U_{dd} = 10\,\text{eV}$, $U_{pp} = 5\,\text{eV}$, and take different values of U_{pd} ranging from $U_{pd} = 0\,\text{eV}$ to $U_{pd} = 3.5\,\text{eV}$. The choice of U_{dd} value is motivated from constraint random phase (cRPA) calculations, which gives $U_{dd}^{\text{cRPA}} \approx 9.0$ eV [44]. Such cRPA values are typically smaller than constraint LDA values, which in some cases yields better results in LDA+DMFT calculations. The reason for this is the frequency dependence of the U_{dd}^{cRPA} which can be actually translated to a Bose factor renormalization of the bandwidth [45]. To the best of our knowledge, for U_{pd} and U_{pp} no reliable estimates are yet available in the literature, but it is certainly a reasonable assumption that these interactions need to be smaller than U_{dd}. The obtained spectral functions are shown in figure 2. As in the bandstructure plots, the color of the spectral function codes the orbital character. Let us start from the spectrum for $U_{pd} = 0$ eV which is plotted in the top left panel. Although the parameters $U_{dd} = 10$ eV and $U_{pp} = 5$ eV are by no means small compared to the bandwidth, we observe a rather uncorrelated spectral function which resembles the non-interacting DOS (figure 1) except for the LHB located below −10 eV. The main reason for this is that, due to the *d–p* hybridization, the filling of each band and, in particular of the *d*-band, is far from an integer value. Upon increasing the value for U_{pd} this hybridization decreases, as can be seen in the spectra, since the charge transfer from *d*-states to *p*-states is now connected with a potential shift of the respective states of the order of U_{pd}. Eventually, with increasing values of U_{pd}, we observe a metal-to-insulator transition. From $U_{pd} = 1.5$ eV to $U_{pd} = 2$ eV most of the spectral weight of the central quasiparticle peak at the Fermi level ($\omega = 0$) is lost. There still remains a residual spectral weight in the gap which eventually goes away from $U_{pd} = 2$ eV to 2.5 eV.

The low-energy gap in figure 2 is between between *d*-states, i.e. an 'upper Hubbard band' with some *p*-hybridization above the Fermi energy ε_F, *and* a mixed *d–p* peak around −2 eV (for $U_{pd} = 2$ eV) or −3 eV (for $U_{pd} = 2.5$ eV). The 'lower Hubbard band' is quite broad and located below ∼−10 eV, whereas most of the *p*-spectral weight is located in a large peak around −4 eV ($U_{pd} = 2$ eV) and −5 eV ($U_{pd} = 2.5$ eV). For $U_{pd} = 3.5$ eV, the *p*-bands are shifted to such low energies that they approach the lower Hubbard bands and start hybridizing with them. Let us emphasize that the formation of the narrow peak at E_F and the transfer of spectral weight to the lower and upper Hubbard bands occurring between 2 and 2.5 eV is a dynamical effect beyond static mean field, as witnessed by the strong ω-dependence of Σ (see figure 5). In summary, DMFT+Hartree yields an insulating state for the original 0MTO parameters *without* the artificial enhancement of the *d–p* splitting hitherto employed in the literature. Instead, we assumed a finite value of U_{pd} which, *in a self-consistent way*, leads to a suppression of *d–p* hybridization driving the metal-to-insulator transition. Yet, we should remark two issues: since 0MTO was designed to reproduce the cuprate bands only around the Fermi energy [35], it is questionable if the 0MTO really yields a good basis for a study of excitations on an energy scale of some eV above and below the Fermi energy such as the *d–p* interplay. We hence present DMFT+Hartree results of the 1MTO model in the following.

1MTO model. As mentioned above, the $N = 1$ orbitals are less localized, and consequently have somewhat longer-ranged hoppings than the $N = 0$ orbitals in order to reproduce the band structure on a larger energy range. Hence, also the corresponding 1MTO values of the local U_{dd} and U_{pp} interaction parameters should be reduced. Concurrently, we find that the 1MTO yields much more *metallic solutions*. The system remains metallic even for the same interaction parameters as we used for the $N = 0$ model in figure 2; to obtain an insulating ground state one needs a larger U_{dd} or U_{pd}.

In figure 3 we show the DMFT+Hartree spectral functions for the $N = 1$ model at $U_{dd} = 13$ eV, $U_{pp} = 7$ eV, and varying U_{pd}. Increasing U_{pd} beyond 3 eV opens a gap in the spectral function However, $U_{dd} = 13$ eV is at the upper edge or larger than the physically reasonable parameter range.

Nature of the mixed d–p peak. As shown in figures 2, 3 a peak of mixed *d*- and *p*-orbital character develops in the $\vec{k}$-integrated spectral functions around −3 eV (for 0MTO at

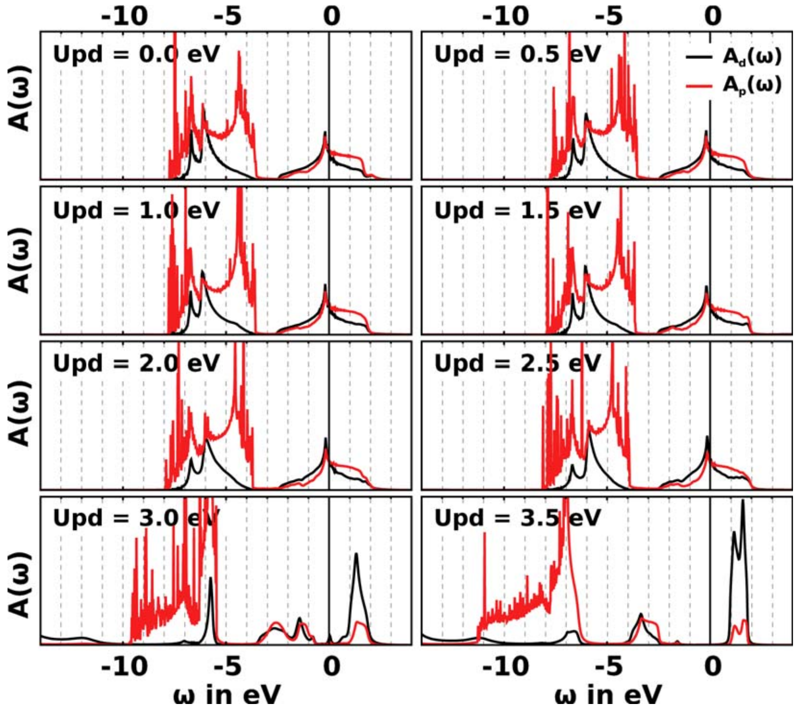

Figure 3. DMFT spectra for the 1MTO basis with interaction parameters $U_{dd} = 13$ eV, $U_{pp} = 5$ eV, and varying U_{pd}; the line at $\omega = 0$ denotes the Fermi level. We have not broadened the δ-peaks with an additional Lorentzian broadening. The only broadening is due to the intrinsic finite lifetime from Im Σ. Please note that there is spectral weight down to -20 eV in the lower two panels which we cut off.

$U_{pd} = 2.5$ eV and 1MTO at $U_{pd} = 3.5$ eV). This peak can be interpreted[6] as a Zhang–Rice state in agreement with previous LDA+DMFT studies [46–48].

In order to see whether or not this spectral weight is also associated to a coherent excitation we calculate $A(\vec{k}, \omega)$ just before and after the metal–insulator transition, i.e. $U_{pd} = 2$–2.5 eV for 0MTO and $U_{pd} = 3$–3.5 eV for 1MTO. The results are shown in figure 4, and the corresponding local d-self-energies are shown in figure 5. Interestingly, the coherence of the spectral feature around -3 eV changes dramatically across the metal–insulator transition for both 0MTO (the two lower panels of figure 4) and 1MTO (the two upper panels). In the two left panels of figure 4, i.e. before the metal–insulator transition, the dispersive band between -3 eV and -1 eV is very incoherent whereas in the two right panels, i.e. just after the metal-insulating transition, a very well defined quasiparticle excitation emerges. The double-occupancies of the d-orbital and the spectral weight at the Fermi level as a function of U_{pd} shows the following: the values of U_{pd} for which the double-occupancies (not-shown) get suppressed are those for which most of the

[6] Note that DMFT allows for the description of a singlet state between the d-site and the bath electrons of the associated Anderson impurity model. In the specific case considered, as it is typically done, the dynamical Weiss field of DMFT effectively includes also the p-degrees of freedom, which are therefore not explicitly separated. The strong mixing among d- and p-orbitals observed at -3 eV, however, supports the intepretation of the corresponding spectral feature as Zhang–Rice state.

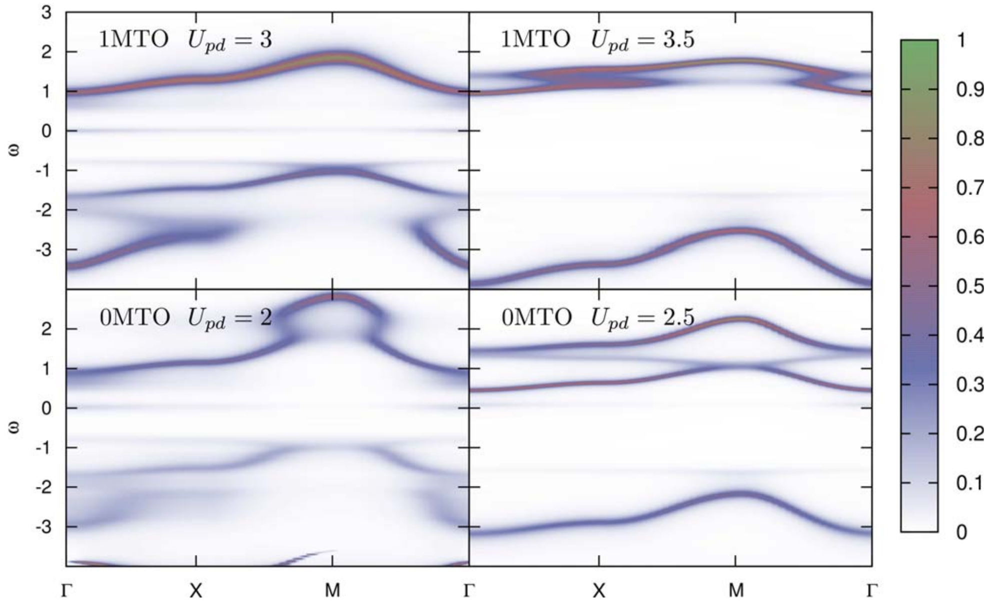

Figure 4. $\vec{k}$-resolved spectral function of 0MTO in the lower and the 1MTO in the upper row. The two left panels are before the charge transfer metal-insulator transition (i.e. for U_{dd} = 10 eV, U_{pp} = 5 eV, U_{pd} = 2 eV and U_{dd} = 13 eV, U_{pp} = 7 eV, U_{pd} = 3 eV in the lower and upper row, respectively). The two right columns are after the metal-insulator transition (obtained by increasing U_{pd}-parameter by 0.5 eV; keeping the other parameters fixed). For both models the mixed *pd*-state becomes suddenly coherent as soon as we enter the insulating state.

spectral weight gets shifted away from the Fermi level. In this strongly-correlated metallic solution an additional peak of mixed *dp* character is formed when a residual finite fraction of itinerant electrons is still present. This spectral feature, which can be interpreted as the emergent Zhang–Rice excitation, becomes more coherent only when the spectral weight at the Fermi level is completely depleted. This depletion, i.e. the opening of the gap, occurs in a similar way as in the Mott–Hubbard transition of the Hubbard model: a pole in the real part of the self-energy develops, see the blue (dashed) lines in figure 5 at $\omega \sim -1.5$ eV. At the same time, the imaginary part of the self-energy develops a peak. This pole respectively peak separates the Zhang–Rice from the upper Hubbard band. There is a second pole in the real part and peak in the imaginary part of the self-energy of figure 5 which splits off the lower Hubbard band and which is located at ~ -7 eV(0MTO, U_{pd} = 2 eV) to ~ -11 eV (1MTO, U_{pd} = 3.5 eV), i.e. between Zhang–Rice singlet and lower Hubbard band. This two pole (peak) structure due to the Zhang–Rice singlet is different from the usual Mott–Hubbard insulator which only has a single pole (peak).[7] Let us emphasize that in our case, the low-energy gap is between *d*-states above and *p*-states below the Fermi level; we have a charge transfer insulator [1] with a Zhang–Rice singlet.

[7] While the two peaks dominate the imaginary part of the self-energy, there is still some imaginary part of the self-energy (scattering) e.g. in the upper Hubbard bands, which gets suppressed with increasing correlations (U_{pd}).

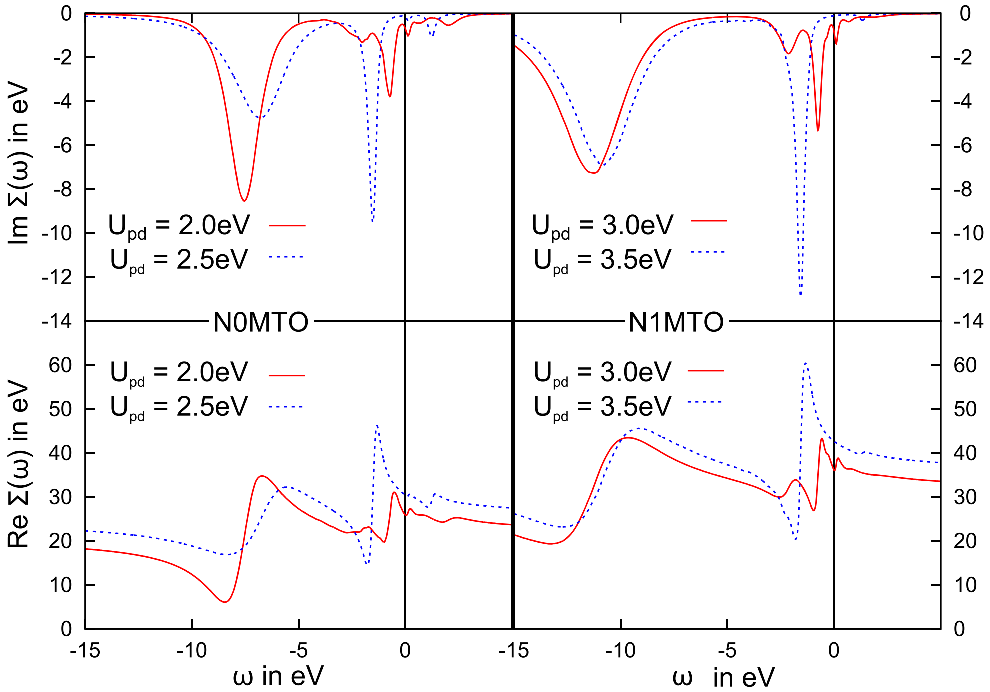

Figure 5. The imaginary (upper panels) and real part (lower panels) of the local DMFT *d*-self-energy on the real axis for the four cases plotted in figure 4.

5. Conclusions

Presently, within the state-of-the art LDA+DMFT calculations, the splitting between the *d*- and *p*-states in cuprates [35] and other transition metal oxides is adjusted for obtaining agreement with experiment, see e.g. [49], or new DC are introduced, see [50]. This is quite unsatisfactory since it basically destroys the often claimed *ab initio* character of the calculation. The aim of our work was hence (i) to understand the physical origin behind such adjustments, and (ii) to perform calculations based on the original parameters from NMTO downfolding *without* artificially changing them. In particular, if the orbital overlap is large, the non-local oxygen–copper interaction U_{pd} can be strong. We have shown that the inclusion of this interatomic interaction is indeed extremely important, because it allows for the description of a *self-consistently determined d–p level splitting*. This mechanism can explain why previous LDA +DMFT calculations that only included the *d–d* interaction yielded—in some cases—poorer results than corresponding studies in smaller *d*-only basis-set. The artificial *p–d* shifts that were employed in the literature actually mimic the effect of U_{pd}. The DMFT+Hartree approach with the explicit inclusion of U_{pd}, adoped in this work, is much more satisfactory from both a practical and a conceptual point of view. The DMFT+Hartree treatment can be based entirely on interaction parameters determined *ab initio* for the downfolded basis-set chosen, e.g. by means of cRPA [51] or its recently developed locally unscreened version [52]. Since the Hartree contribution of U_{pd} is its leading contribution in the limit of many neighbors and since it yields, as we have seen, an important *p–d* level shift it should be included in future LDA+DMFT calculations that include the oxygen p levels. Beyond that also screening effects of U_{pd} might be relevant. These could be more easily included in *GW*+DMFT.

For the specific case of undoped cuprates, the two downfolded models considered, 0MTO and 1MTO, qualitatively yield the same physics, see figures 2–4. Quantitatively, the results for the 1MTO model require somewhat larger interaction parameters than 0MTO to open an insulating gap. For 0MTO we have a charge transfer insulator for plausible interaction parameters, whereas for 1MTO these are at the borderline or even somewhat larger than expected [44]. Let us note in this respect that non-local interactions, beyond the realm of our DMFT+Hartree treatment, also play an important role for cuprates and will further stabilize the insulating solution. Also in the paramagnetic phase these non-local correlations will reduce the critical interactions for the metal-to-insulator transition [17, 53].

Let us emphasize that the impact of our analysis goes well beyond the particular, though significant case of the insulating phase in undoped cuprates. In fact, for other transition metal oxides with a more three dimensional crystal and electronic structure, non-local correlations beyond DMFT are less important, except for low temperatures [13, 14]. Hence, one can expect a DMFT+Hartree calculation including *ab initio* the U_{pd} interaction to be sufficient for capturing the physics of downfolded d–p models which are nowadays fixed by hand [49]. In practice, similarly as for the Emery model, the U_{pd} interactions will turn the physics of the dp-model towards that of the d-only model, because the number of d-electrons is reduced towards an integer value, entailing stronger electronic correlations. Our paper hence paves the way for better treatment of oxygen p-orbitals in LDA+DMFT calculations.

Acknowledgments

We acknowledge very helpful discussions with O K Andersen and T Saha-Dasgupta as well as L Vaugier, P Seth and S Biermann. We also would like to thank F F Assaad for providing us with the maxent code. AT benefited from financial support by the Austrian Science Fund (FWF) through research unit FOR 1346 (FWF project ID I597); KH from the FWF SFB ViCoM F41. GS acknowledges support by the Deutsche Forschungsgemeinschaft (FOR 1162). Calculations have been done on the Vienna Scientific Cluster.

Appendix

Analytic continuation. To obtain high quality spectra with as little ambiguity as possible we employ the continuation of the self-energy scheme as described in [41]. Compared to the more often used continuation of the Green function, the continuation of the self-energy has the advantage of leading to guaranteed physical self-energies, since the condition of positivity of the imaginary part of the self-energy is incorporated in the maximum entropy method (maxent). Furthermore, compared to the maxent for the Green functions, this scheme has the advantage of avoiding an unnecessary maxent-step for the p-bands, whose self-energy is known and constant. This way maxent is applied only to the part beyond Hartree of the correlated orbitals, whereas all other quantities, e.g. $H_{\vec{k}}$ and the Hartree self-energy Σ_{H} can be treated exactly on the real axis. In the practical implementation, we measure the Green's function from a converged run directly in Matsubara frequencies $i\omega_n$ to avoid binning errors as would be the case when

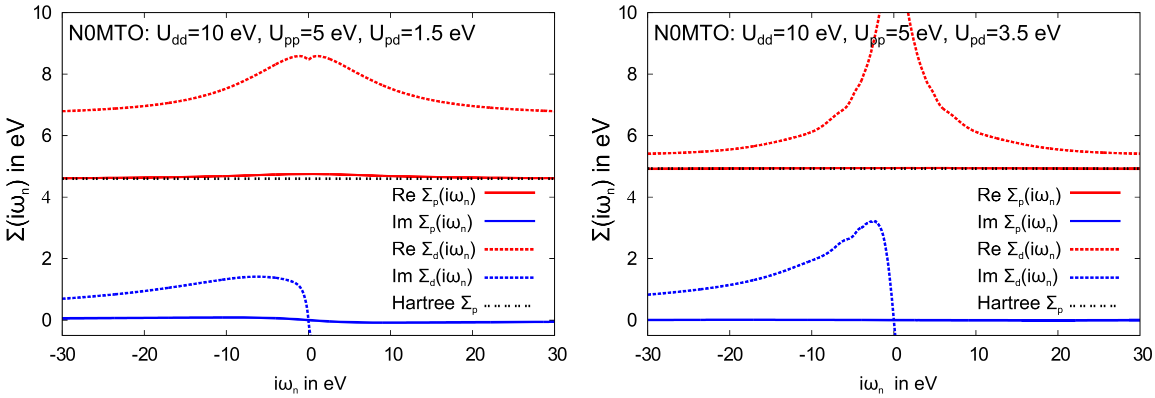

Figure 6. Local DMFT self-energy of the *p*-orbitals compared to the corresponding Hartree calculation for the 0MTO Emery model with $U_{pd} = 1.5(3.5)$ eV, $U_{pp} = 5$ eV, $U_{dd} = 10$ eV in the left (right) panel. For both cases the Hartree self-energy of the *p*-orbitals is almost identical to the one which was calculated with the CTQMC.

measuring the Green's function in imaginary time τ. Then we calculate the self-energy $\Sigma(i\omega_n)$ using the Dyson equation $\Sigma(i\omega_n) = \mathcal{G}_0^{-1}(i\omega_n) - G^{-1}(i\omega_n)$, assuming that the bath Green's function $\mathcal{G}_0^{-1}$ does not contain statistical errors. To calculate the error for the self-energy we employ the bootstrap method on 300 independent Green's function measurements. The self-energy has a different asymptotic behavior from that of the Green's function. The latter is however needed for maxent-like methods. Therefore a manipulation of the input is needed. To this end one performs a high-frequency expansion of the CTQMC self-energy which for the single band Hubbard model reads:

$$\begin{aligned}\Sigma_\sigma(i\omega_n) &= U_{dd}\langle n_{-\sigma}\rangle \\ &\quad + U_{dd}^2\langle n_{-\sigma}\rangle(1 - \langle n_{-\sigma}\rangle)(i\omega_n)^{-1} + O\left((i\omega_n)^{-2}\right).\end{aligned} \tag{3}$$

Following the argument above and with the knowledge that the Green's function has a $1/(i\omega_n)$ asymptotic behavior, we subtract the Hartree term for the *d*-band, $U_{dd}\langle n_{-\sigma}\rangle$ and divide the remaining part of the self-energy by the prefactor of the $1/(i\omega_n)$ term. This new object, $\widetilde{\Sigma}(i\omega_n)$, can then be analytically continued to the real axis by means of the stochastic maxent method [42, 43].

In this respect, by inspecting the correlation matrix of the self-energy we checked that different Matsubara frequencies are uncorrelated, otherwise a transformation to a non-correlated basis would have been necessary. We finally calculated the spectral function, $A(k, \omega)$, from $\widetilde{\Sigma}(\omega)$ and all other terms, namely the DC correction, the $\vec{k}$-dependent Hamiltonian $H_{\vec{k}}$, the chemical potential μ and the Hartree self-energy of Σ_{H}:

$$\begin{aligned}A_\sigma(\vec{k}, \omega) &= -\frac{1}{\pi}\,\mathrm{Im}\left[\omega + \mu - DC - H_{\vec{k}} - \Sigma_{\mathrm{H}}\right. \\ &\quad \left. -\widetilde{\Sigma}(\omega)U_{dd}^2\langle n_{-\sigma}\rangle(1 - \langle n_{-\sigma}\rangle)\right]^{-1}.\end{aligned} \tag{4}$$

To test the validity of our approach we also compared data of an ED-calculation with data obtained by our CTQMC implementation, which resulted in very good agreement.

DMFT(CTQMC) for the p-electrons. Here, we validate that a Hartree treatment of U_{pp} is sufficient. To this end we performed for some test calculations where both U_{dd} and U_{pd} are treated in DMFT, and U_{pd} in Hartree, which actually is the correct (full) DMFT treatment of the Emery model. Figure 6 shows the obtained DMFT self-energy, which is basically the same as the Hartree self-energy. For $U_{pd} = 1.5$ eV, very minor deviations are discernible at low frequencies, but the Hartree self-energy is still an accurate approximation of the DMFT self-energy. Therefore, we conclude that a Hartree treament of U_{pp} is absolutely sufficient.

References

[1] Zaanen J, Sawatzky G A and Allen J W 1985 *Phys. Rev. Lett.* **55** 418
[2] Imada M, Fujimori A and Tokura Y 1998 *Rev. Mod. Phys.* **70** 1039–263
[3] Bednorz J G and Müller K A 1986 *Z. Phys* B **64** 189
[4] Hubbard J 1963 *Proc. R. Soc. Lond.* A **276** 238
Gutzwiller M C 1963 *Phys. Rev. Lett.* **10** 159
Kanamori J 1963 *Prog. Theor. Phys.* **30** 275
[5] Metzner W and Vollhardt D 1989 *Phys. Rev. Lett.* **62** 324
[6] Georges A and Kotliar G 1992 *Phys. Rev.* B **45** 6479
[7] Georges A, Kotliar G, Krauth W and Rozenberg M 1996 *Rev. Mod. Phys.* **68** 13
[8] Anisimov V I, Poteryaev A I, Korotin M A, Anokhin A O and Kotliar G 1997 *J. Phys.: Condens. Matter* **9** 7359
Lichtenstein A I and Katsnelson M I 1998 *Phys. Rev.* B **57** 6884
Kotliar G, Savrasov S Y, Haule K, Oudovenko V S, Parcollet O and Marianetti C A 2006 *Rev. Mod. Phys.* **78** 865
Held K 2007 *Adv. Phys.* **56** 829
[9] See, e.g. Hansmann P, Toschi A, Sangiovanni G, Saha-Dasgupta T, Lupi S, Marsi M and Held K 2013 *Phys. Status Solidi* B **250** 1251–64 and references therein
[10] Hettler M H, Tahvildar-Zadeh A N and Jarrell M 1998 *Phys. Rev.* B **58** 7475(R)
Maier T, Jarrell M, Pruschke T and Keller J 2000 *Phys. Rev. Lett.* **85** 1524
Kotliar G, Savrasov S Y, Pálsson G and Biroli G 2001 *Phys. Rev. Lett.* **87** 186401
Lichtenstein A I and Katsnelson M I 2000 *Phys. Rev.* B **62** 9283(R)
Maier T A, Jarrell M, Pruschke T and Hettler M H 2005 *Rev. Mod. Phys.* **77** 1027
[11] Rubtsov A N, Katsnelson M I and Lichtenstein A I 2008 *Phys. Rev.* B **77** 033101
Hafermann H, Li G, Rubtsov A N, Katsnelson M I, Lichtenstein A I and Monien H 2009 *Phys. Rev. Lett.* **102** 206401
Toschi A, Katanin A and Held K 2007 *Phys. Rev.* B **75** 045118
Held K, Katanin A A and Toschi A 2008 *Prog. Theor. Phys. Suppl.* **176** 117
Slezak C, Jarrell M, Maier Th and Deisz J 2009 *J. Phys.: Condens. Matter* **21** 435604
Rohringer G, Toschi A, Hafermann H, Held K, Anisimov V I and Katanin A A 2013 *Phys. Rev.* B **88** 115112
[12] Gull E, Ferrero M, Parcollet O, Georges A and Millis A J 2010 *Phys. Rev.* B **82** 155101
[13] Katanin A A, Toschi A and Held K 2009 *Phys. Rev.* B **80** 075104
Rohringer G, Toschi A, Katanin A and Held K 2011 *Phys. Rev. Lett.* **107** 256402
[14] Fuchs S, Gull E, Pollet L, Burovski E, Kozik E, Pruschke T and Troyer M 2011 *Phys. Rev. Lett.* **106** 030401
Gull E, Staar P, Fuchs S, Nukala P, Summers M S, Pruschke T, Schulthess T C and Maier T 2011 *Phys. Rev.* B **83** 075122

[15] Molegraaf H J A *et al* 2002 *Science* **295** 2239
Boris A *et al* 2004 *Science* **304** 708
Ortolani M, Calvani P and Lupi S 2005 *Phys. Rev. Lett.* **94** 067002
[16] Toschi A, Capone M, Ortolani M, Calvani P, Lupi S and Castellani C 2005 *Phys. Rev. Lett.* **95** 097002
Toschi A and Capone M 2008 *Phys. Rev.* B **77** 014518
[17] Comanac A, de' Medici L, Capone M and Millis A J 2008 *Nature Phys.* **4** 287
[18] Nicoletti D *et al* 2010 *Phys. Rev. Lett.* **105** 077002
[19] Parragh N, Toschi A, Held K and Sangiovanni G 2012 *Phys. Rev.* B **86** 155158
[20] Werner P, Comanac A, de Medici L, Troyer M and Millis A J 2006 *Phys. Rev. Lett.* **97** 076405
[21] Rubtsov A N and Lichtenstein A I 2004 *JETP Lett.* **80** 61
[22] de' Medici L, Wang X, Capone M and Millis A J 2009 *Phys. Rev.* B **80** 054501
Wang X, de Medici L and Millis A J 2010 *Phys. Rev* B **81** 094522
[23] Weber C, Haule K and Kotliar G 2008 *Phys. Rev.* B **78** 134519
[24] Andersen O K, Saha-Dasgupta T, Tank R W, Arcangeli C, Jepsen O and Krier G 1999 ed H Dreysse *Lecture Notes in Physics* (Berlin: Springer)
Andersen O K and Saha-Dasgupta T 2000 *Phys. Rev.* B **62** R16219
Andersen O K, Saha-Dasgupta T, Ezhov S, Tsetseris L, Jepsen O, Tank R W and Krier C A G 2001 *Psi-k Newsl.* **45** 86
[25] See, e.g. Poteryaev A I, Tomczak J M, Biermann S, Georges A, Lichtenstein A I, Rubtsov A N, Saha-Dasgupta T and Andersen O K 2007 *Phys. Rev.* B **76** 085127
Saha-Dasgupta T, Lichtenstein A and Valenti R 2005 *Phys. Rev.* B **71** 153108
Jakobi E, Kanungo S, Sarkar S, Schmitt S and Saha-Dasgupta T 2011 *Phys. Rev.* B **83** R041103
Pavarini E, Biermann S, Poteryaev A, Lichtenstein A I, Georges A and Andersen O K 2004 *Phys. Rev. Lett.* **92** 176403
[26] Han M J, Wang X, Marianetti C A and Millis A J 2011 *Phys. Rev. Lett.* **107** 206804
Wang X, Han M J, de' Medici L, Park H, Marianetti C A and Millis A J 2012 *Phys. Rev.* B **86** 195136
[27] Hansmann P, Toschi A, Yang X, Andersen O K and Held K 2009 *Phys. Rev. Lett.* **103** 016401
Hansmann P, Toschi A, Yang X, Andersen O K and Held K 2010 *Phys. Rev.* B **82** 235123
[28] Parragh N, Sangiovanni G, Hansmann P, Hummel S, Held K and Toschi A 2013 *Phys. Rev.* B **88** 195116
[29] For a recent systematic LDA+DMFT analysis of Ni-heterostructures, also see Rüegg A, Hung H-Hs, Gull E and Fiete G A 2013 arXiv:1310.5818
[30] Emery V J 1987 *Phys. Rev. Lett.* **58** 2794–7
[31] Zhang F C and Rice T M 1988 *Phys. Rev.* B **37** 3759–61
[32] Andersen O K, Liechtenstein A I, Jepsen O and Paulsen F 1995 *J. Phys. Chem. Solids* **56** 1573–91
[33] Pavarini E, Dasgupta I, Saha-Dasgupta T, Jepsen O and Andersen O K 2001 *Phys. Rev. Lett.* **87** 047003
[34] Saha-Dasgupta T, Nuss J, Jepsen O and Andersen O K 2009 unpublished
[35] Kent P R C, Saha-Dasgupta T, Jepsen O, Andersen O K, Macridin A, Maier T A, Jarrell M and Schulthess T C 2008 *Phys. Rev.* B **78** 035132 see the discussion on page 3 left column
[36] Vaugier L *PhD Thesis* Ecole Polytechnique, Paris (in preparation)
[37] de'Medici L, Georges A and Biermann S 2005 *Phys. Rev.* B **72** 205124
[38] Weber C, Haule K and Kotliar G 2008 *Phys. Rev.* B **78** 134519
[39] Anisimov V I, Zaanen J and Andersen O K 1991 *Phys. Rev.* B **44** 943
[40] Müller-Hartmann E 1989 *Z. Phys.* B **74** 507
Müller-Hartmann E 1989 *Int. J. Mod. Phys.* B **3** 2169
Müller-Hartmann E 1989 *Z. Phys.* B **76** 211
[41] Wang X, Gull E, Medici L, Capone M and Millis A J 2009 *Phys. Rev.* B **80** 045101
[42] Beach K S D 2004 arXiv:cond-mat/0403055
[43] Abendschein A and Assaad F F 2006 *Phys. Rev.* B **73** 165119
[44] Hansmann P, Vaugier L and Biermann S private communication

[45] Casula M, Werner P, Vaugier L, Aryasetiawan F, Miyake T, Millis A J and Biermann S 2012 *Phys. Rev. Lett.* **109** 126408
[46] Yin Q, Gordienko A, Wan X, Savrasov S Y, Weber C, Haule K and Kotliar G 2008 *Phys. Rev. Lett.* **100** 066406
[47] Weber C, Haule K and Kotliar G 2010 *Nature Phys.* **6** 574–8
[48] Wang X, de' Medici L and Millis A J 2011 *Phys. Rev.* B **83** 094501
[49] Dang H T, Millis A J and Marianetti C A 2013 arXiv:1309.2995
[50] Haule K, Birol T and Kotliar G 2013 arXiv:1310.1158
[51] Aryasetiawan F, Imada M, Georges A, Kotliar G, Biermann S and Lichtenstein A I 2004 *Phys. Rev.* B **70** 195104
[52] Nomura Y, Kaltak M, Nakamura K, Taranto C, Sakai S, Toschi A, Arita R, Held K, Kresse G and Imada M 2012 *Phys. Rev.* B **86** 085117
[53] Rost D, Gorelik E V, Assaad F and Blümer N 2012 *Phys. Rev.* B **86** 155109
Park H, Haule K and Kotliar G 2008 *Phys. Rev. Lett.* **101** 186403